GA–A23822

# ECH COMES OF AGE FOR MAGNETIC FUSION RESEARCH

by
J. LOHR, S.W. DELAWARE, R.W. CALLIS, W.P. CARY, J.C. DeBOO, J.L. DOANE, I. GORELOV, R.J. LA HAYE, H.J. GRUNLOH, C.C. PETTY, R.I. PINSKER, D. PONCE, R. PRATER, and S.G.E. PRONKO

APRIL 2002

## DISCLAIMER

GA–A23822

# ECH COMES OF AGE FOR MAGNETIC FUSION RESEARCH

by
J. LOHR, S.W. DELAWARE, R.W. CALLIS, W.P. CARY, J.C. DeBOO, J.L. DOANE, I. GORELOV, R.J. LA HAYE, H.J. GRUNLOH, C.C. PETTY, R.I. PINSKER, D. PONCE, R. PRATER, and S.G.E. PRONKO

This is a preprint of a paper presented at the 19th IEEE/NPSS Symposium on Fusion Engineering, January 21–25, 2002 in Altantic City, New Jersey and to be published in the *Proceedings.*

Work supported by
the U.S. Department of Energy under
Contract No. DE-AC03-99ER54463

GA PROJECT 30033
APRIL 2002

# ECH Comes of Age for Magnetic Fusion Research

J. Lohr, S.W. Delaware, R.W. Callis, W.P. Cary, J.C. DeBoo, J.L. Doane, I. Gorelov, R.J. La Haye, H.J. Grunloh, C.C. Petty, R.I. Pinsker, D. Ponce, R. Prater, and S.G.E. Pronko

*General Atomics, P.O. Box 85608, San Diego, California 92186-5608*

**Abstract—Advances in gyrotron technology are resulting in new capabilities and scientific results on magnetic confinement devices for fusion research worldwide. Unit output power of 1 MW and higher, at frequencies greater than 100 GHz and quasi-cw operation have become possible. This has led to successful experiments on electron cyclotron heating, electron cyclotron current drive, non-inductive tokamak operation, tokamak energy transport, suppression of instabilities and advanced profile control leading to enhanced performance. The synthetic diamond gyrotron output window is being developed as the answer to the requirement for a low loss blocking window with excellent thermal and mechanical properties and the potential for cw operation at high power. Ancillary equipment for efficient microwave transmission over distances of hundreds of meters, polarization control, diagnostics and flexible launch geometry have all been developed and proven in regular service.**

**There now is excellent convergence between the experimental measurements and theoretical understanding of the heating and current drive mechanisms. The reliability of high power gyrotron installations is at the level previously achieved by neutral beam systems.**

## I. INTRODUCTION

The scientific motivation for development of high power long pulse gyrotron tubes for fusion research is that tokamak parameters can be increased by control of the current density profile, that plasma instabilities can be stabilized by precisely applied heating and current drive, and that a reactor eventually will need to be operated steady state. Because of the efficiency of electron cyclotron current drive, the small size of the microwave beam and the strong resonant absorption, these requirements can all be met by high power long pulse gyrotron oscillators [1] operating at the electron cyclotron resonance or its harmonics. The toroidal magnetic field in a tokamak is given as a function of the major radius by

$$B = 2\times10^{-7}\, NI/R \ (T) \quad , \tag{1}$$

where N is the number of turns in the toroidal field coil, I is the current and R is the distance from the torus center. The electron cyclotron frequency is,

$$\omega = qB/\gamma m \quad , \tag{2}$$

where q is the electronic charge, m is the electron mass and gamma is the relativistic factor. To first order, ω is inversely proportional to R in the case of the tokamak. The same equation (2) holds in the uniform magnetic field of the gyrotron cavity where it determines the output microwave frequency of the device.

In the simplest version of the gyrotron [2], a cylindrical electron beam accelerated to 10 s of keV and confined by an axial magnetic field passes through a cylindrical copper cavity close to the copper wall. If the cavity Q is high, and if an electric field which initially grows from noise is present, strong pumping of a cavity eigenmode occurs. The cavity dimensions, the diameter of the cylindrical electron beam and the magnetic field determine the mode.

The rf energy in the high order cavity mode, for example the $TEM_{22,6,1}$ mode used in the CPI gyrotrons at DIII–D or the $TEM_{19,5,1}$ mode used in the Gycom gyrotrons, is converted to a Gaussian beam and separated from the electron beam by a Vlasov convertor as modified by Denisov [3,4]. The convertor is a part of the cavity with a spiral cutout which forms the rf energy into a Gaussian beam by providing the proper phase delay so that, as the rf energy escapes from the cavity, planar phase fronts are established. The rf beam, propagating obliquely to the electron beam, is reflected from a series of mirrors, which can be custom formed both to focus the beam to a Gaussian waist and to provide slight phase corrections. At or near the Gaussian waist a blocking window separates the high vacuum inside the gyrotron from the outside world. The blocking window must pass the full rf beam power with relatively low loss. Sapphire, boron nitride and, most recently, CVD diamond have been used as windows in the gyrotrons at DIII–D. Although diamond in principle offers an ideal solution to the problem of window material selection, there has been a learning process, which will be discussed below, in its development.

In the general application of gyrotron generated microwaves to fusion research, the rf beam is focused by mirrors to a second waist at the input to waveguide, to a Gaussian optical relay system, or to a hybrid line and transported to the tokamak. The line contains diagnostic devices, polarization control mirrors, dummy loads and other components to permit characterization and low loss transmission over distances up to 100 m [5]. Gyrotron development has resulted in high power devices at frequencies up to 170 GHz, permitting the second harmonic of the electron cyclotron frequency in the tokamak to be used. This increases the accessible density to about $7\times10^{19}/m^3$ before cutoff is reached for B = 2 T. Transmission effiency for 100 m is about 80%.

The application of EC power to tokamaks will be motivated in the next section by a summary of the major scientific results to date. Although gyrotron technology is at least adolescent, if not fully mature, a number of new developments are being pursued which will enhance the utility of these devices while decreasing the cost per watt. Some of these developmental activities will be discussed. Finally, the plans

for the future on the DIII–D tokamak, particularly as they relate to the application of electron cyclotron technology, will be presented.

## II. SCIENTIFIC RESULTS

### *A. Transport*

The adjective "surgical" is often used to describe the precision with which electron cyclotron heating and current drive can be applied to a tokamak plasma. In DIII–D the rf beams have diameters of about 10 cm at the tokamak center and power is absorbed over about 5 cm radially. This precision has made possible several experiments both to characterize and to exploit the efficiency of heating and current drive.

The ability to modulate the ECH power and to seek a response in the electron channel has been used to study electron transport. An example of such an experiment is shown in Fig. 1, in which the power is deposited at a specific location, heating the electrons locally, and diffusing radially at a rate determined by the local electron transport coefficient. The EC injection was perpendicular to the toroidal magnetic field to eliminate current drive effects and provide the best spatial localization of the heating. The electron cyclotron emission (ECE) diagnostic measures the local electron temperature at a number of spatial points on both sides of the deposition region. Fitting an exponential to the time response of $T_e$ at different radii for square wave modulation yields the spatial profile of the electron energy confinement time and this in turn gives the transport coefficient.

A second transport experiment investigated the heat pinch phenomenon. Heating in the center of the discharge increases the peak electron temperature and approximately scales the entire profile at constant form factor. When heating is applied off-axis, one expects a shoulder to form in the profile and a more constant temperature to be observed inside the heating location. The actual observation is that the central temperature also increases and that the profile maintains a relatively constant shape with larger average value as shown in Fig. 2. This result indicates that, for the off-axis case, the energy flowed against the temperature gradient, a phenomenon dubbed "heat pinch." A slightly negative heat flux inside the heating location is inferred from the data. The stiffness of the electron temperature profile shape in tokamaks has long been a subject of interest and conjecture. The detailed diagnostic measurements of profiles, the increased precision of transport calculations and the ability of electron cyclotron heating to put

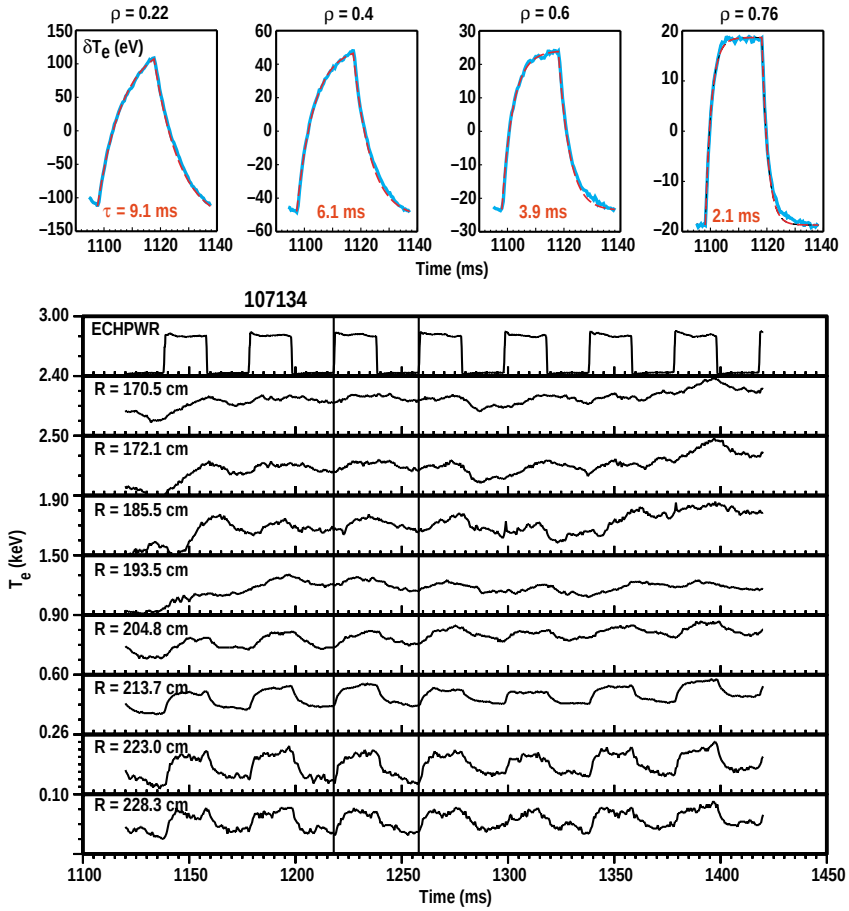


Fig. 1. The rf power, about 2.0 MW modulated at 25 Hz, was deposited close to the plasma edge at R ~ 220 cm. The effect on the electron temperature can be seen throughout the plasma with a slight phase shift for locations far from the deposition location. The shape of the heating effect gives directly the local incremental confinement time. Perpendicular rf injection was used to localize the deposition.

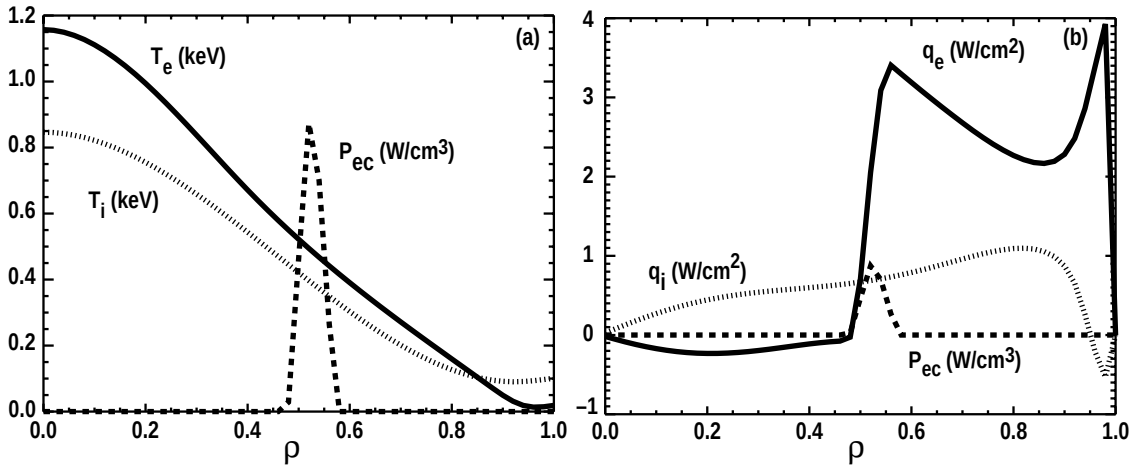


Fig. 2. In this experiment the rf power was applied at a normalized radius of about 0.52, nevertheless the electron temperature profile remained peaked. A transport analysis using the measured deposition profile and kinetic profiles shows that the heat flux in the electron channel is slightly negative inside the deposition location, in opposition to diffusive flow.

substantial power into a small and controllable volume should greatly facilitate investigations of this counter-intuitive phenomenon.

*B. Current Drive*

Tokamak performance is a strong function of the current density profile. The same precision with which electron cyclotron heating can be applied provides the opportunity to control j(r) using electron cyclotron current drive, with the critical advantage that, unlike the usual inductively driven currents with j(r) profiles determined transiently by current diffusion, the control can be applied continuously.

The process works because of the spatial dependence of the cyclotron frequency and the Doppler shift. For injection of electron cyclotron waves off-perpendicular to the magnetic field from the low field side, the waves will be at a frequency above the local cyclotron frequency, calculated from (2), until they reach the resonance. Electrons moving toward the wave direction encounter a Doppler shifted resonance outside the cold resonance and are heated preferentially. The collisionality of these electrons therefore decreases with the result that a localized positive current flows in the opposite direction, the direction of the wave injection. This current can be used to stabilize a class of instabilities or to provide the optimum j(r) profile for advanced tokamak operation.

The current drive efficiency for electron cyclotron waves is very good in the plasma center, where the temperature is high and collisionality is low. As the current drive is moved off axis to larger major radii, to locations critical both for advanced tokamak operation and suppression of instabilities, the efficiency begins to decrease faster than would be expected from the decrease in electron temperature alone. The efficiency remains high when the current drive is moved inboard of the magnetic axis on the plasma midplane.

Trapped electron orbits are primarily on the outboard side of the magnetic axis. Trapped particles can limit the off-axis current drive to values which might be too low for effective use of the ECCD. It began to be seen, however, that the low field off-axis current drive efficiency increased when the plasma beta, the ratio of plasma pressure to magnetic field pressure, began to increase. These results are summarized in Fig. 3., where the normalized current drive efficiency remains relatively constant as the interaction region is moved outboard for high beta, high performance H–mode plasmas.

The explanation for this effect can be seen from the phase space diagram in Fig. 4. Electrons are heated in a region of phase space which depends on their velocity distribution function. An electron which receives a boost in perpendicular energy from the wave can be moved up in phase space to lie within the trapping boundary. Such electrons can no longer carry current, with the result that the current drive efficiency drops rapidly as the resonance is shifted further and further off-axis.

But increasing the electron beta moves the absorption further from the trapping boundary, with the result that a kick in perpendicular energy does not move the electrons up into the trapping region and the current drive efficiency remains

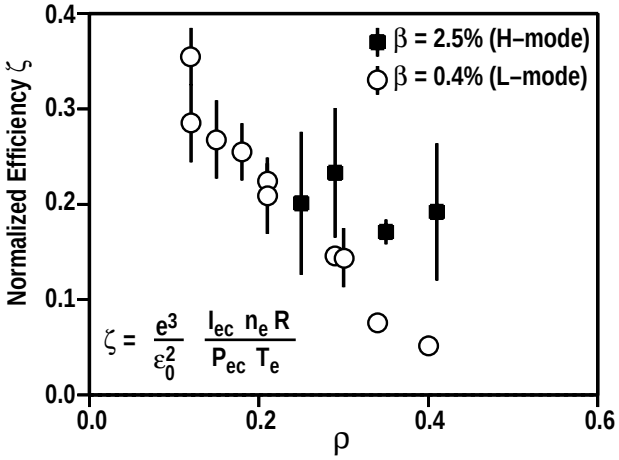


Fig. 3. At low beta, the current drive efficiency drops as a function of ECCD location both due to decrease in electron temperature and particle trapping. The trapping effect is nearly eliminated for high beta operation.

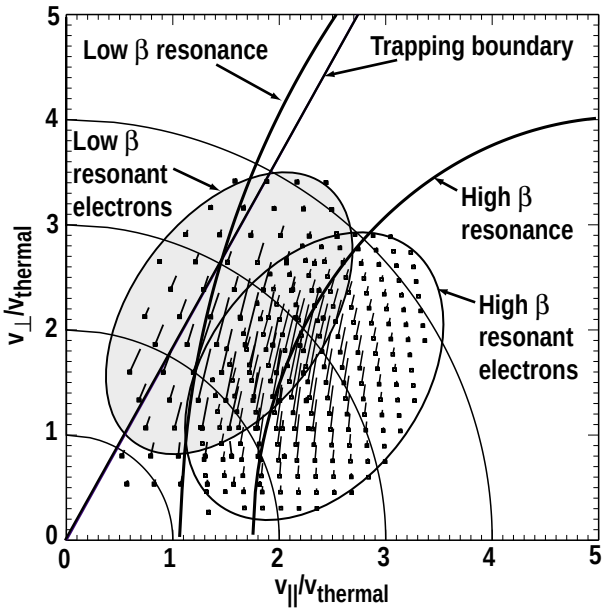


Fig. 4. At high beta, the resonant electrons do not cross the trapping boundary and are not lost from the current carriers. Thus the current drive efficiency remains high.

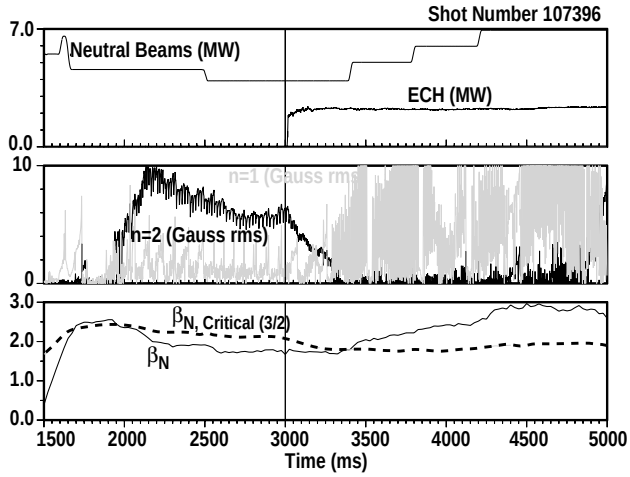


Fig. 5. The m/n=3/2 tearing mode was completely suppressed by precisely applied electron cyclotron current drive. Following suppression, the plasma beta was increased by increasing the NBI power without a return of the 3/2 NTM. The 2/1 mode, which replaced the 3/2 mode, was not as dissruptive and may be able to be suppressed when higher ECCD power is available.

high, nearly constant, as a function of radius. Maximum driven currents of 120 kA have been measured on DIII–D with excellent agreement between the measurements and the Fokker-Planck theory, including trapping and residual electric fields. Current profile control leading to enhanced tokamak performance parameters is therefore well within the realm of possibility. Increased power levels should provide increased current drive with good flexibility.

### *C. Stabilization of Instabilities*

The neoclassical tearing mode arises when the bootstrap current, which is driven by the electron pressure gradient in a magnetic geometry having the radial dependence given in (1) is locally reduced, for example, due to local fluctuations at a rational q surface. Once the bootstrap current, which locally can be a substantial fraction of the total, is reduced, a magnetic island forms, across which the transport can be rapid, producing a deterioration of confinement. Simply restoring the current can, in principle, restore the plasma confinement to its original value, perhaps even allowing an increase in the achievable average beta in the process. The magnitude of the driven current must be about equal to the local bootstrap current, which is well within the capability of the DIII–D ECH system at measured current drive efficiencies for the m/n=3/2 rational surface.

Complete stabilization of the 3/2 neoclassical tearing mode has been demonstrated. In Fig. 5 the mode, detected by magnetic search coils, is shown to be completely suppressed by application of ECCD exactly at the island location. The current drive location has been varied both by scanning the magnetic field and by a rigid body shift of the entire plasma. Both experiments indicate that a precision of about a centimeter in the current drive location is required. In this demonstration of instability control, the precision of control of the current drive location and the high efficiency, when trapping is avoided by driving current on the high field side of the magnetic axis, are both critical elements. Upon stabilization of the mode, higher electron betas could be achieved by increasing the neutral injection power. Stabilization of the m/n=2/1 mode, was not achieved at the 2.2 MW power level available to date.

## III. HARDWARE DEVELOPMENTS

### *A. Diamond Windows*

Until recently, the gyrotron output window has imposed a critical limit on the power, pulse length and efficiency of gyrotrons. Boron nitride, for example, has a temperature limit of about 1000°C, which translates to a limit of about 800 kW at 2.0 s pulses for 4% absorption. Sapphire, which has about 10 times lower absorption, has such poor thermal conductivity that it must be face cooled, implying double disk windows and chloro-fluorocarbon coolants which pose a variety of risks for the gyrotron and the tokamak in case of window failure. In addition, the peak power limitations for these materials required the gyrotron designers to spread the output beam as it passes through the window. It has proven difficult to restore the broadened rf beams to Gaussian beams without loss of about 10% of the total rf power.

The development of chemical vapor deposition (CVD) technology for production of high purity synthetic diamond windows [6] has changed the situation dramatically. Artificial diamond (Fig. 6), can have a loss tangent at 110 GHz even lower than $1\times10^{-5}$ which implies an absorption of less than 0.2% for the typical thicknesses needed. CVD diamond also has thermal conductivity of 6.5 kW/m$^2$K, about four times greater than copper, so edge cooling is a viable option. With CVD diamond, the possibility of cw operation at 1.0 MW or higher has become a reality. Several problems were


Fig. 6. Photograph of two CVD diamond disks. The smaller has diameter 60 mm and thickness 0.55 mm. The larger is 73 mm diameter and 1.7 mm thick. Typical loss tangents at 110 GHz are $< 5\times10^{-5}$ for these disks.

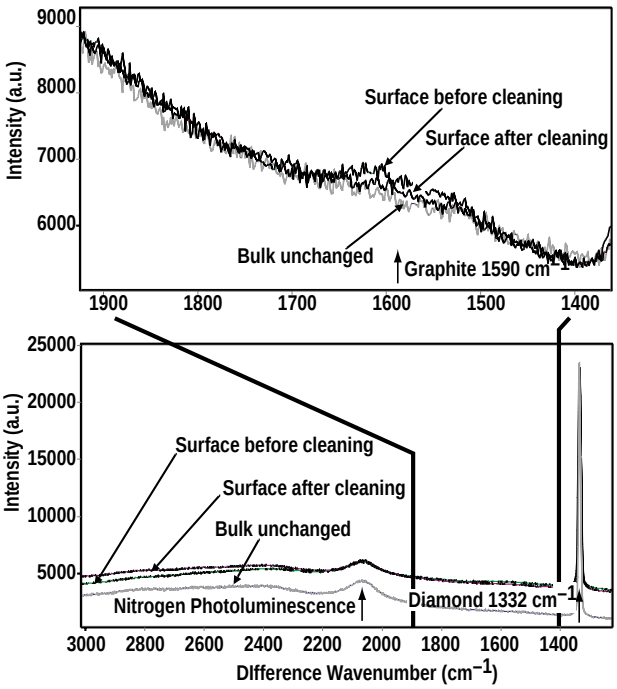


Fig. 7. Raman scattering spectra for CVD diamond windows showing contamination, indicated by the graphite bond at 1590 $cm^{-1}$. The feature at 2060 $cm^{-1}$ is tentatively identified as photoluminescence from nitrogen contamination at low concentration. The sharp peak at 1332 $cm^{-1}$ is the diamond signature. Spectra obtained after cleaning by grit blasting with 3 μm alumina show a reduction in surface graphite. The graphite signature deeper in the diamond was unchanged by cleaning, verfying surface contamination.

encountered with the first diamond disks, however, which were linked to the processes whereby the diamond was brazed to flanges and which resulted in the failures of the windows.

The earliest seals were made by an aluminum diffusion bonding process. This resulted in direct contact between the aluminum and the cooling water, which, despite precautions, resulted in corrosion of the seals and subsequent vacuum failure. In at least one case, a window with aluminum seal failed catastrophically at relatively low power due to hydrogen contamination, which may have arisen during the braze process.

An Au/Cu braze has been developed, which promises to solve the corrosion problem, however some of the first examples of window assemblies produced using this process exhibited absorption up to eight times greater than anticipated, probably due to carbon contamination of the surfaces during brazing. Several windows with this contamination also failed catastrophically. As a result, new quality control steps are being instituted in which Raman scattering is being used to check for contamination of the diamond, particularly by graphitic carbon, and loss tangent measurements are being performed at several laboratories at a number of points in the production process, rather than just after the production of the bare disk. Typical Raman scattering spectra made using an argon laser pump at 514 nm are shown in Fig. 7 for a diamond sample contaminated with carbon and exhibiting the graphite peak at 1590 $cm^{-1}$ and a peak at 2060 $cm^{-1}$ tentatively identified as photo-luminescence from nitrogen contamination at low concentration. Also shown are spectra from the contaminated sample after cleaning by grit blasting with 3 μm alumina. The first gyrotrons produced using these additional proof checks are just coming into operation. The safety margin below the yield stress of about 350 MPa for these windows is a factor of three.

*B. Dummy Loads*

A dummy load must be able to absorb the full output power of the gyrotron, which could be 1–1.5 MW cw, while at the same time providing a completely black absorber with very low reflected power. Although this has proved to be difficult in the past, excellent dummy loads are now available which meet the requirements. In one solution, a rotating mirror scans the rf beam over a water cooled surface coated with a graded layer of $TiO_2$. This load is capable of true cw operation and provides unmeasurable reflections [7]. It can be operated both in air and vacuum and is compatible with waveguide and quasi-optical transmission systems.

Another load, applicable to systems using evacuated corrugated waveguide, uses a smooth waveguide section and tapered corrugation depth to convert the incident $HE_{1,1}$ waveguide mode to lossy surface modes, which are damped on the water cooled walls of the guide [8]. This load absorbs about 80% of the incident power and must be backed by a simple low power load, which can, however, be somewhat reflective, since reflected power will be completely absorbed during the second pass through the mode conversion section. A mode conversion load is shown installed on a 110 GHz gyrotron in Fig. 8. These loads have the advantage of avoiding rotating seals and are quite compact, simply replacing a 2 m

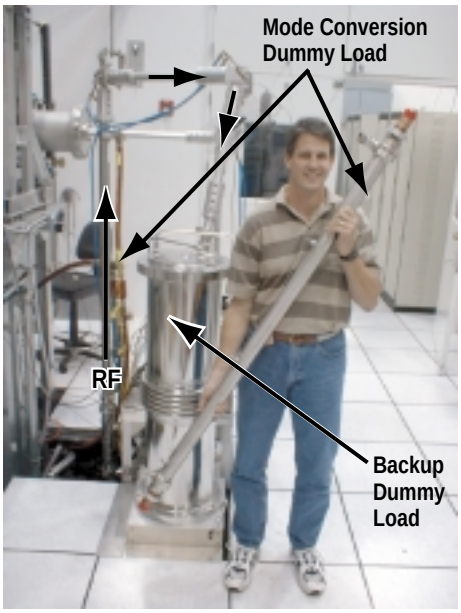


Fig. 8. Photograph of a mode conversion dummy load for 110 GHz. The load is very black and absorbs about 80% of the incident power and 100% of the power reflected back through it.

section of standard waveguide, but must incorporate a waveguide bellows section to accommodate the 2–4 mm thermal expansion of the absorbing section.

*C. Polarization Control*

For the low field side launch of the rf power at the second harmonic of the electron cyclotron frequency, the extraordinary mode must be generated [9]. For injection perpendicular to the total magnetic field, X–mode will have linear polarization with the **E** vector perpendicular to the magnetic field. For current drive, however, the injection is oblique. To couple to the X–mode for this case requires that the incident rf beam be elliptically polarized. A millimeter wave system for tokamak heating and current drive must, therefore, incorporate flexible control of the the elliptical polarization. This is done in the DIII–D system using two grooved mirrors mounted in miter bends with remote control of the direction of the grooves with respect to the plane of the bend.

A typical waveguide line in the DIII–D system can be up to 100 m in length and contains up to 11 miter bends. The polarization miters can be located in any of the bends, although typically one with grooves having depth of about $\lambda/2$ is used first to rotate the plane of the linearly polarized wave. This is followed by one with $\lambda/4$ gooves to give elliptical polarization [10]. A computer code, which takes into consideration the plasma equilibrium, the variable launcher geometry and the specifics of a particular transmission line, determines the polarizer angles to be used for any specific experimental requirement.

The polarization of the launched rf beam can be determined by direct measurements using a polarimeter with a rotating quarter wave plate [11] or can be inferred from the plasma response to modulated rf injection. The power deposition profile will be very localized for pure X–mode and will be broader and centrally peaked for O–mode. Mixed polarization will yield a superposition of the two characteristics. Measurements of the linear polarization for the DIII–D system made at the last miter bend before the launcher showed better than 95% of the power was in the desired polarization for several combinations of polarizer angles.

*D. Launcher Antennas*

The ability to scan the injected rf beam in a poloidal plane is necessary to take full advantage of the localized heating and current drive capability of the ECH system. Additionally, experiments to investigate current drive in both the co- and the counter-current directions or heating only require flexibility in setting the toroidal injection angle. Each of the DIII–D launcher assemblies [12], shown in Fig. 9, can deliver the output from two gyrotrons and incorporate both these mechanical degrees of freedom. The launcher mirrors presently can be moved between tokamak pulses, but a real-time motion is under consideration.

Each launcher has a fixed focusing mirror and a flat steering mirror for each waveguide line. These mirrors are not actively cooled, although they dissipate approximately 0.5% of the incident energy, therefore ratcheting temperatures are a possibility. The mirrors must be designed so that eddy current forces are not excessive during disruptive plasma events. Two designs are presently being used. One employs an OFHC solid copper mirror with a relatively thin reflecting surface, a thicker central region providing thermal inertia and an emitting back surface to cool the mirror by radiation to the low temperature surroundings. A second design features a multilayer copper/stainless steel laminate to reduce eddy currents and provide thermal inertia and conductance and radiation to the cooled support structure. These two designs will be characterized at full power during the next experimental campaign.

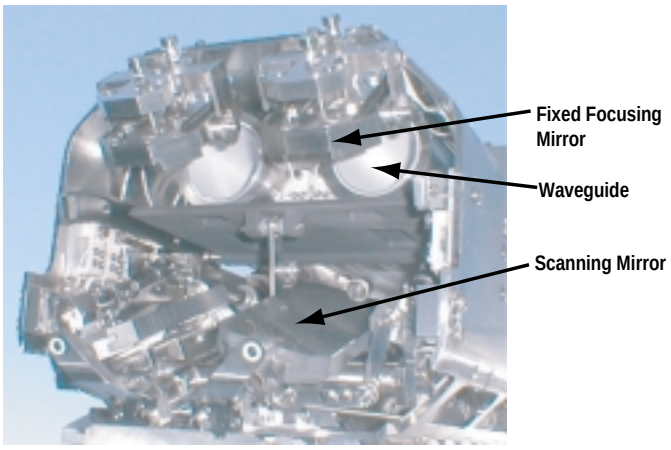


Fig. 9. The launchers are capable of handling 1.0 MW from each of two waveguides for pulse lengths up to 5 s and can scan both poloidally and toroidally. The mirrors are radiatively cooled.

## IV. FUTURE PLANS

Experiments to date have indicated that increased power and pulse length will be required fully to exploit the advantages of ECH/ECCD for tokamak operation. The DIII–D tokamak has available ports for four dual launcher assemblies, which would, with gyrotron upgrades, permit the injected power to be tripled for pulse lengths of 5–10 s. A development program is now creating a design for a 1.5 MW gyrotron in which recovery of some of the energy in the collected electron beam results in an increase in the rf production efficiency from the present 30% to about 50%. Short pulse tests of the gun are being conducted at MIT while design and construction of the collector are projects of Calabazas Creek Research. The DIII–D program is planning to advance to a six gyrotron system using the existing designs for the 2002 campaign.

## V. CONCLUSION

ECH systems capable of generating single unit power levels near 1.0 MW for pulse lengths of several seconds are now being installed and operated on tokamak devices at several laboratories around the world. The first scientific results have verified the efficacy of these systems for heating and current drive leading to advanced tokamak operation and control of instabilities. The ancillary systems to provide integrated transmission and control of the rf beams have been developed and are routinely available. New research and development will increase the unit output power by about 50% at higher rf production efficiency. The DIII–D program should have a six gyrotron system available for the 2002 campaign with over 3.0 MW injected rf power.

## ACKNOWLEDGMENT

This work was supported by the U.S. Department of Energy under Contract DE-AC03-99ER54463.

## REFERENCES

[1] The gyrotron oscillators in use at the DIII–D tokamak are manufactured by *CPI,* Palo Alto California and by *Gycom*, Nizhny Novgorod, Russia.

[2] A.V. Gaponov, M.I. Petelin and V.K. Yulpatov, *Radiophys. Quantum Electron,* **10,** 794 (1967).

[3] M. Blank, K. Kreischer and R.J. Temkin, *IEEE Trans. Plasma Sci.*, **PS-24**, 1058 (1996).

[4] G.G. Denisov, A.N. Kuftin, V.I. Malygin, N.P. Venedictov, and V.E. Zapevalov, *Int J. Electronics,* **72,** 1079 (1992).

[5 J. Lohr, D. Ponce, R.W. Callis, J.L. Doane, H. Ikezi and C.P. Moeller, *Proc. 23rd Int. Conf on Infrared and Millimeter Waves,* University of Essex, Colchester, Essex, UK, 269 (1998).

[6] K. Takahashi, K Sakamoto, A. Kasugai, T. Imai, J.R. Brandon and R.S. Sussmann, *Rev. Sci. Instruments,* **71,** 4139 (2000).

[7] R. Lawrence Ives, Max Mizuhara, Richard Schumacher, and Rand Pendleton, *IEEE Trans. Plasma Sci.*, **27,** No. 2 (1999).

[8] John L. Doane, *Int. J. Infrared and Millimeter Waves,* **14,** 363 (1992).

[9] F.M.A. Smits, *Proc. of the Eighth Joint Workshop on Electron Cyclotron Emission and Electron Cyclotron Resonanance Heating,* Gut Ising, Germany, Max Planck Institut fur Plasmaphysik, **II**, 549 (1993).

[10] J.L. Doane, *Int. J. Infrared and Millimeter Waves,* **13,** 1727 (1992).

[11] H. Ikezi, C.P. Moeller, J.L. Doane, M. DiMartino, J. Lohr, D. Ponce, and R.W. Callis, Rev. Sci. Instrum. **68**, 478 (1998).

[12] The articulating launchers were designed and built by Princeton Plasma Physics Laboratory.